The Journal of Experimental Biology 213, 339-346
Published by The Company of Biologists 2010
doi:10.1242/jeb.036947

The role of granules within viscous capture threads of orb-weaving spiders

B. D. Opell* and M. L. Hendricks

Department of Biological Sciences, Virginia Polytechnic Institute and State University, Blacksburg, Virginia 24061, USA

*Author for correspondence (bopell@vt.edu)

Accepted 7 October 2009

SUMMARY

Sticky viscous prey capture threads form the spiral elements of spider orb-webs and are responsible for retaining insects that strike a web. These threads are formed of regularly spaced aqueous droplets that surround a pair of supporting axial fibers. When a thread is flattened on a microscope slide a small, opaque granule can usually be seen within each droplet. These granules have been thought to be the glycoprotein glue that imparts thread adhesion. Both independent contrast and standard regressions showed that granule size is directly related to droplet volume and indicated that granule volume is about 15% of droplet volume. We attempted to find support for the hypothesized adhesive role of granules by establishing an association between the contact surface area and volume of these granules and the stickiness of the viscous threads of 16 species in the context of a six-variable model that describes thread stickiness. However, we found that granule size made either an insignificant or a small negative contribution to thread stickiness. Consequently, we hypothesize that granules serve to anchor larger, surrounding layers of transparent glycoprotein glue to the axial fibers of the thread, thereby equipping droplets to resist slippage on the axial fibers as these droplets generate adhesion, elongate under a load, and transfer force to the axial fibers.

Key words: adhesion, Araneoidea, capture thread, glue, glycoprotein, orb-web.

INTRODUCTION

The sticky prey-capture threads in orb-webs constructed by over 4500 spider species (Platnick, 2009) retain insects, giving a spider more time to locate, run to, and subdue them by wrapping them with silk or injecting them with venom (Chacón and Eberhard, 1980; Eberhard, 1986; Eberhard, 1990; Blackledge and Eliason, 2007). These threads account for the largest part of an orb-web's silk length and mass (Eberhard, 1986; Townley et al., 2006) and are spun by spiders belonging to two Orbiculariae subclades (Coddington and Levi, 1991; Griswold et al., 1998; Griswold et al., 2005; Blackledge et al., 2009). The Deinopoidea clade comprises spiders that, like their non-orb-weaving ancestors, produce dry, cribellar capture threads formed of thousands of fine, dry protein fibrils that surround a pair of supporting axial fibers (Peters, 1984; Peters, 1986, Peters, 1992; Eberhard and Pereira, 1993; Opell, 1994a; Opell, 1994b; Opell, 1996; Opell, 1999). Members of the much larger Araneoidea clade produce moist, viscous capture threads with axial fibers that support regularly spaced aqueous droplets (Fig. 1) (Peters, 1986; Vollrath et al., 1990; Vollrath and Tillinghast, 1991; Vollrath, 1992; Tillinghast et al., 1993).

Viscous threads are the product of three spigots found on each of an araneoid spider's paired posterior lateral spinnerets. A single flagelliform gland spigot produces an axial fiber and is flanked by two aggregate gland spigots, which cover the fiber with aqueous material. The products of the two spinnerets merge to produce a pair of axial fibers enclosed in a sheath of viscid material, which forms into a series of droplets that differ greatly size and spacing among species (Fig. 1). This viscous material contains hydrophilic compounds that attract atmospheric moisture and maintain droplet volume (Vollrath et al., 1990; Townley et al., 1991). This water causes the axial fibers to supercontract, shortening their lengths, increasing their tension (Work, 1981; Work, 1982; Savage and Gosline, 2008; Gosline et al., 1994), and, thereby, ensuring that viscous threads are taut and better equipped to recruit the adhesion generated by multiple viscous droplets (Opell and Hendricks, 2007; Opell and Hendricks, 2009; Opell et al., 2008).

When a viscous thread is placed on a microscope slide, a small opaque granule is usually visible at the center of each of the larger, primary droplets on the thread (Fig. 2) and often also within the smaller secondary droplets that lie between the primary droplets of many species (Fig. 1). However, granules are not visible within suspended droplets (Fig. 1). These granules are thought to be the glycoprotein glue that is found within droplets and confers a thread's stickiness (Vollrath and Tillinghast, 1991; Tillinghast et al., 1993; Peters, 1995). Glycoprotein glue is retained by araneoids of the family Theridiidae that have evolved cob-webs (Hu et al., 2007).

If granules contain the glycoprotein that is responsible for thread adhesion we must ask why a granule should constitute such a small portion of a droplet's volume and what role the remaining volume plays. The non-granule volume seems much greater than required to impart supercontractility to axial fibers, although it could be required to deliver the precursors of the central granule. Moreover, when thread stickiness is measured (e.g. Opell and Hendricks, 2007) droplets at the edge of contact with a surface extend to such a degree that it is difficult to understand how a droplet's granule would have sufficient volume to form a central adhesive filament that could lie within the elongating droplet (Fig. 3).

Here, we quantitatively examine the hypothesized contribution of granules to viscid thread stickiness. We do this by attempting to reject the null hypothesis that the size of granules is insignificantly or negatively correlated with thread stickiness. We test this hypothesis in the context of a previous study that modeled the contributions of six thread variables to the stickiness that threads of 16 araneoid species registered on contact plates of four widths (Opell and Hendricks, 2009). In the current study we first attempt to show that flattened granule contact surface area or granule volume is an acceptable substitute for the droplet size variable that makes a highly significant and positive contribution to thread stickiness in

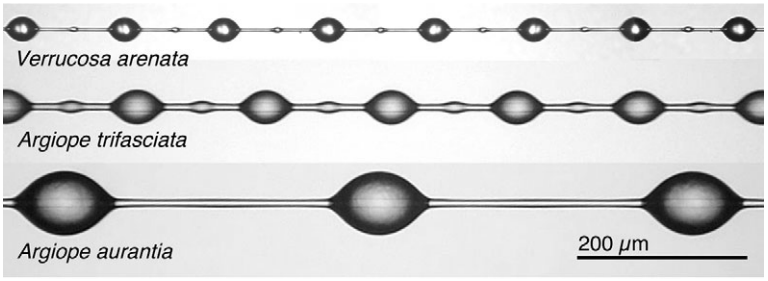

Fig. 1. Suspended viscous capture threads of three araneoid species.

the previous study. Following this, we attempt to show that, when added to the six-variable model, the total granule surface area associated with a contact plate or the total granule volume associated with a contact plate makes a significant and positive contribution to modeled thread stickiness. We also use independent contrast analyses to examine the relationship between granule size and viscous droplet volume in a phylogenetic context and then describe significant relationships in standard regression models.

MATERIALS AND METHODS

Species studied and thread collection

We collected threads from newly spun orb-webs constructed by adult females of 17 Araneoidea species: one species from the family Theridiosomatidae: *Theridiosoma gemmosum* (L. Koch); three species from the family Tetragnathidae: *Meta ovalis* (Gertsch), *Leucauge venusta* (Walckenaer) and *Tetragnatha elongata* Walckenaer; and 13 species from the family Araneidae: *Micrathena gracilis* (Walckenaer), *Micrathena sagittata* (Walckenaer), *Argiope aurantia* Lucas, *Argiope trifasciata* (Forskål), *Metepeira labyrinthea* (Hentz), *Larinioides cornutus* (Clerck), *Cyclosa turbinata* (Walckenaer), *Verrucosa arenata* (Walckenaer), *Neoscona crucifera* (Lucas), *Araneus pegnia* (Walckenaer), *Araneus bicentenarius* (McCook), *Araneus marmoreus* Clerck, and *Mangora maculata* (Keyserling). Threads of *Meta ovalis* and *Araneus bicentenarius* were collected from forests at the base of Grandfather Mountain, Avery Co., NC, USA. Threads of the other species were collected from sites within 10 km of Blacksburg, Montgomery Co., VA, USA. *Neoscona crucifera* was not included in a previous study (Opell and Hendricks, 2009) because we did not measure the water content of this species' droplets. However, we included *N. crucifera* in the independent contrast and regression analysis of the current study.

We collected web sectors on 15 cm diameter rings with 5 mm wide rims and 5 mm wide center bars that were covered with double-sided Scotch® tape (Tape 665; 3M Co., St Paul, MN, USA) to hold thread strands securely. In the laboratory we collected viscous threads on samplers made by gluing raised supports to microscope slides, as described by Opell and Hendricks (Opell and Hendricks, 2007; Opell and Hendricks, 2009). Double-sided tape also covered these supports and maintained thread tension. These samplers permitted us to photograph threads under a compound microscope and then to measure their stickiness.

Summary of previously measured thread features

The methods used to characterize threads and model their stickiness are described in detail by Opell and Hendricks (Opell and Hendricks, 2009). Therefore, we summarize these methods and describe in detail only the methods for measuring glycoprotein granules and examining their association with thread stickiness and droplet volume.

After photographing suspended threads we cleaned and placed a new glass coverslip onto the supports of a microscope slide sampler. Upon contacting a coverslip, the droplets of the suspended thread sectors between the supports flattened against the coverslip and their granules became visible (Fig. 2). We used ImageJ (http:/rsb.info.nih.gov/ij/index.html) to measure the dimensions and spacing of suspended primary and secondary thread droplets and the dimensions of granules in flattened primary droplets. The granules in secondary droplets were too small to be measured accurately.

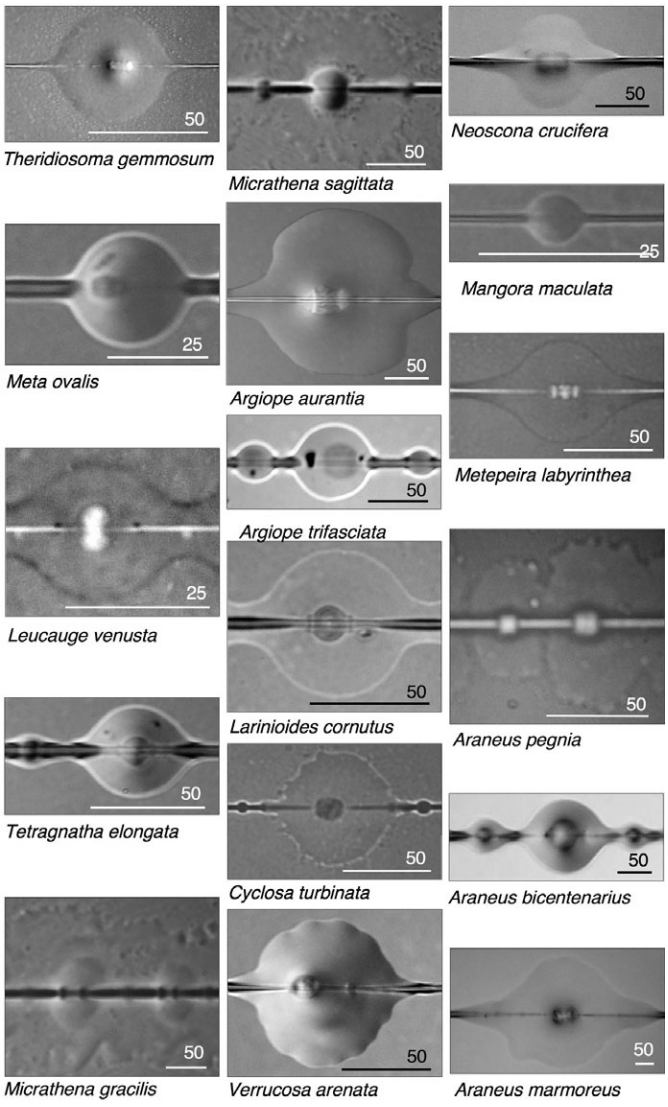

Fig. 2. Droplets of viscous capture threads flattened against a coverslip to show granules near the center of each droplet.

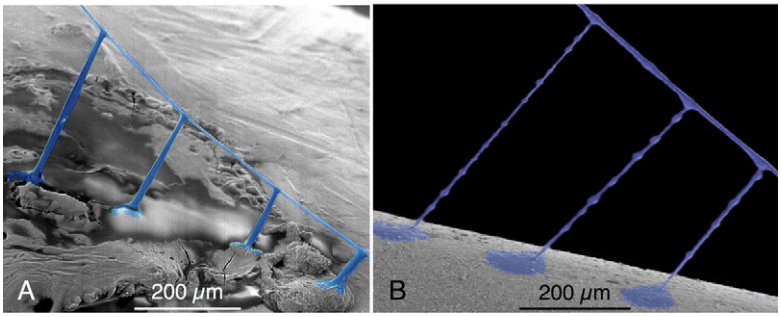

Fig. 3. Scanning electron micrographs of *A. trifasciata* viscous threads in early (A) and late (B) stages of droplet elongation as force is applied to a thread adhering to a surface.

From measurements of suspended droplets we computed the SHAPE of primary droplets as twice the focal length of a parabola defined by the outline of the lower half of a primary droplet. As SHAPE is computed from droplet length and width, it accounts for differences in both droplet size and configuration. From the frequency and distribution of secondary droplets we computed SVPP, the total volume of a species' secondary droplet material associated with each of the contact plates used to measure thread stickiness. These plates had widths of 963, 1230, 1613 and 2133 μm.

From images of flattened threads we measured the combined contact surface areas of primary and secondary droplets in a 1 mm length of thread and multiplied this value by the width in millimeters of each of the four contact plates used to measure thread stickiness, to obtain APP, the contact surface area of flattened primary and secondary droplets associated with a contact plate.

From measurements of droplet images made with a compound microscope on the day that each of the threads was collected and from images of these threads made under the high vacuum of a scanning electron microscope we computed fresh and desiccated droplet volumes, and from these determined PH2O, the proportion of water in an individual's droplets.

We evaluated the extensibility of axial fibers within each species' viscous threads by attaching threads to the open jaws of a digital caliper and slowly separating the jaws until the thread ruptured. Double-sided carbon tape (used for mounting specimens to be examined with a scanning electron microscope) secured threads to bars. We then applied Kores® mimeograph correction fluid (Ink Technology Corp., Tenafly, NJ, USA) along the length of thread spans that contacted the tape. Dividing the final length of a thread by its initial span provides an index that we term residual extensibility (RE). This index is the same as breaking extension and accounts for the extensibility that remains after a spider manipulates its viscous thread during web construction. Although we believe that the combined use of tape and mimeograph correction fluid held the threads securely, it is possible that the viscous material allowed some axial fiber slippage. However, RE had an interspecific range of 3.53 to 9.06, indicating that this index is useful in characterizing the extensibility of threads at their native web tensions.

Viscous threads recruit the adhesion of multiple thread droplets, but they do so imperfectly, with each successively interior droplet contributing progressively less adhesion (Opell and Hendricks, 2007). As a primary droplet contributes 69.93% of the adhesion of the adjacent outer droplet (Opell and Hendricks, 2009), it is possible to compute the effective droplet number (EDN) of a viscous thread span, the total droplet equivalents that contribute to a thread's stickiness as registered by contact plates of each width. For example a span of five droplets would have an EDN of 3.9 (1.0+0.7+0.5+0.7+1.0).

We measured thread stickiness by pressing contact plates of four widths against suspended sectors of each individual's threads at a constant speed until a standard force was achieved. We then withdrew the plate at a constant speed and recorded the maximum

Table 1. Primary droplet and granule size and shape

Species	Modeling group	Primary droplet volume (μm³)	Granule shape	Granule length (μm)	Granule width (μm)	Granule surface area (μm²)	Granule volume (μm³)
Theridiosoma gemmosum	3	1311±959	R (4)	10.6±0.9	3.6±0.2	38.5±4.0	103.1±57.8
Meta ovalis	3	1003±170	E (5)	7.4±1.2	7.3±1.5	48.2±15.5	126.9±31.7
Leucauge venusta	1	769±227	E (2), R (6)	5.0±0.7	7.6±0.6	36.4±6.2	100.8±30.5
Tetragnatha elongata	1	5846±2332	E (4)	14.8±3.4	11.7±2.5	156.7±59.0	853.0±385.9
Micrathena gracilis	2	4105±486	E (2)	26.9±1.1	27.3±1.7	579.6±58.3	1454.5±67.2
Micrathena sagittata	2	4297±896	E (1), R (3)	24.0±4.7	30.9±2.3	701.2±148.1	596.7±150.5
Argiope aurantia	1	63,217±13,821	E (4)	54.3±8.4	38.9±4.1	1790.9±485.1	14,932.7±7648.5
Argiope trifasciata	1	20,625±4969	R (2)	52.0	25.0	880.0±4.0	3391.1±2141.4
Metepeira labyrinthea	1	3621±739	E (3), R (2)	14.8±3.6	11.3±1.7	166.3±61.5	375.4±132.1
Larinioides cornutus	1	20,264±9409	E (2), R (2)	32.9±10.3	15.9±1.3	525.5±216.0	5314.3±3546.9
Cyclosa turbinata	3	516±88	E (4), R (1)	14.1±0.9	12.7±1.4	155.3±39.5	268.8±64.2
Verrucosa arenata	1	5804±1149	E (1), R (2)	16.3±1.1	11.9±1.5	187.6±37.9	646.7±103.9
Neoscona crucifera	–	3708±601	E (3)	20.3±2.6	18.7±3.2	310.8±90.7	856.1±175.4
Mangora maculata	3	4.±0.3	E (2)	3.1±0.8	2.0±0.6	5.3±2.6	2.6±1.1
Araneus pegnia	2	16,716±5363	E (1), R (5)	14.8±1.1	13.5±1.9	204.9±44.0	437.4±138.7
Araneus marmoreus	2	98,109±15,476	E (5), R (5)	51.9±4.0	34.9±2.5	1625.2±173.5	9148.9±2162.2
Araneus bicentenarius	1	43,234±13,694	E (6)	45.3±6.9	42.3±9.4	1748.6±625.8	12,489.0±5845.0

Granule shape: E, elliptical ; R, rectangular; sample size in parentheses.
Values are mean±1 s.e.m.

force that was registered before the plate pulled free of the thread, as registered in μN by the digital read-out of a load cell connected by a lever to the contact plate. Three measurements were made with each individual spider's threads on each contact plate width.

Measuring droplet and granule features

For modeling analyses we use the primary droplet volume (PV) reported by Opell and Hendricks (Opell and Hendricks, 2009). However, the PVs given in Table 1 and used in independent contrast and regression analyses were computed for threads of individuals whose granules were measured and, therefore, for some species, differ slightly from values reported in Opell and Hendricks (Opell and Hendricks, 2009). As in this previous study, we computed PV using the following formula based on a parabola, which most closely matches the profile of viscous droplets:

$$PV = (2\pi DW^2 \times DL) / 15 , \quad (1)$$

where DW is droplet width and DL is droplet length.

We measured the length and width (GL and GW) of the most sharply focused granule in images of an individual's flattened primary droplets and scored the shape of the granule profile as either an ellipse (e.g. *A. trifasciata* and *L. cornutus* in Fig. 2) or a rectangle (e.g. *A. aurantia* and *N. crucifera* in Fig. 2). We computed the contact surface area of the oval granules as:

$$GA = \pi \times ((GL + GW) / 4)^2 , \quad (2)$$

and the contact surface area of the rectangular granules as:

$$GA = GL \times GW . \quad (3)$$

We estimated an individual's granule volume based on two considerations: (1) as a granule is contained within a droplet, the volume of the granule must be smaller than the volume of a droplet; and (2) as a granule appears to be denser than the surrounding viscous material and to extend above this material when a droplet is flattened, the granule is thicker than the rest of the flattened droplet. An estimator of granule volume (GV) that meets these requirements is:

$$GV = GA \times 2T , \quad (4)$$

where T is the mean thickness of the flattened droplet, determined by dividing the measured volume of an individual's suspended primary droplet by the surface area of the flattened primary droplet.

Determining granule indices per contact plate

The total contact surface area and volume of primary droplet granules (GAPP and GVPP, respectively) associated with contact plates used to measure thread stickiness (Table 2) were computed as:

$$GAPP = GA \times PDPP \quad (5)$$

$$GVPP = GV \times PDPP , \quad (6)$$

where PDPP is the number of primary droplets per contact plate, determined by multiplying plate width (in mm) by the number of primary droplets per mm thread length.

Analysis

We used the SAS program (SAS Institute Inc., Cary, NC, USA) to perform the statistical tests reported in this study. Independent contrast analyses were based on a pruned phylogeny of araneoid species from Scharff and Coddington (Scharff and Coddington, 1997) as shown in Fig. 4, with relationships between the three *Araneus* species inferred from female genitalic morphology (Levi, 1971; Levi, 1973). All branch lengths were set to 1 and analyses were performed using the 'Y contrasts *vs* X contrasts (positivized)' option of the PDAP module (Midford et al., 2005) run under the Mesquite 1.06 program (Maddison and Maddison, 2008). We consider a test with $P \leq 0.05$ to be significant.

RESULTS

Granules in the context of a six-variable model of stickiness

We developed the following comprehensive, six-variable regression model (P=0.0001 and R^2=0.88) to describe the stickiness per contact plate (SPP) that 16 species' threads (*N. crucifera* was not included in this model) registered on contact plates of 963, 1230, 1613, and 2133 μm widths (Opell and Hendricks, 2009):

$$SPP = (62.2537EDN) + (15.0522SHAPE) + (0.0020SVPP) - (213.6091PH2O) - (11.4523RE) - (0.0006APP) - 202.3569.$$

In the current study we first attempted to show that flattened granule contact surface area or granule volume (Table 1) was an acceptable substitute for the SHAPE index, which made a highly significant (P=0.0001) and positive contribution to thread stickiness, accounting for about 50% of the modeled thread stickiness. However, neither index of granule size proved to be a satisfactory substitute for SHAPE. When GA was substituted it made a small negative contribution (P=0.04) to SPP, but EDN and RE became insignificant (P=0.20 and 0.13, respectively). When these insignificant variables were removed GA itself became insignificant

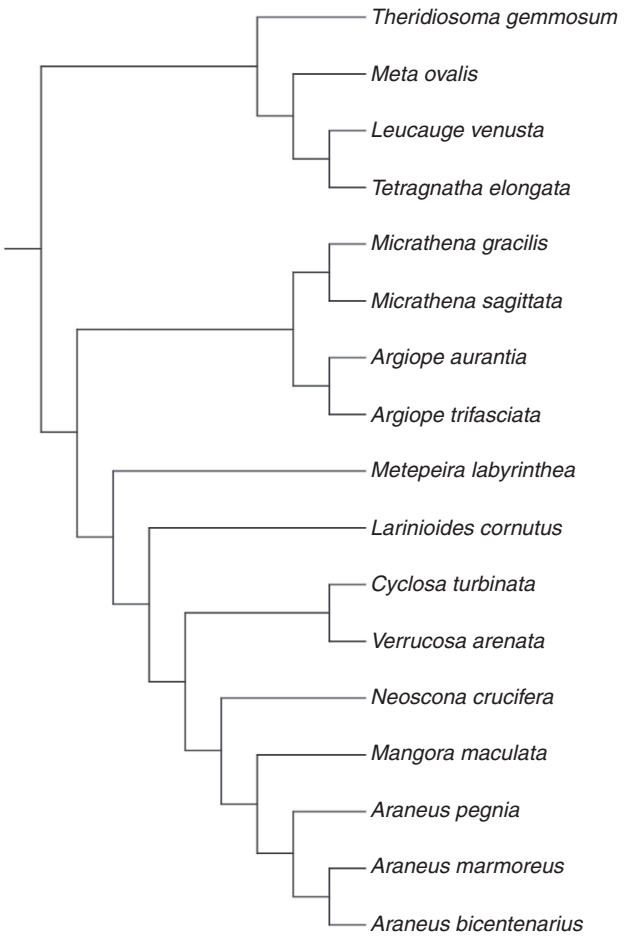

Fig. 4. Phylogeny of araneoid species included in this study, taken from Scharff and Coddington (Scharff and Coddington, 1997); with relations among *Araneus* species inferred from Levi (Levi, 1971; Levi, 1973).

Table 2. Total granule number, surface area and volume per contact plate used to measure thread stickiness

Species (*N*)	Granules per plate*	Granule surface area per plate (μm^2)	Granule volume per plate (μm^3)
Theridiosoma gemmosum (4)	10.6; 13.5; 17.7; 23.5	408; 521; 683; 904	1092; 1395; 1829; 2418
Meta ovalis (5)	19.8; 25.3; 33.2; 43.9	955; 1220; 1600; 2094	2517; 3215; 4216; 5518
Leucauge venusta (8)	28.7; 36.7; 48.1; 63.6	1045; 1335; 1750; 2314	2892; 3693; 4843; 6405
Tetragnatha elongata (4)	12.5; 16.0; 21.0; 27.7	1961; 2505; 3285; 4344	10,679; 13,640; 17,887; 23,654
Micrathena gracilis (2)	9.5; 12.2; 16.0; 21.1	5526; 7058; 9256; 12,240	13,867; 17,711; 23,226; 30,713
Micrathena sagittata (4)	11.0; 14.0; 18.4; 24.3	7698; 9832; 12,893; 17,050	6550; 8366; 10,971; 14,508
Argiope aurantia (4)	3.4; 4.3; 5.6; 7.5	6037; 7710; 10,111; 13371	50,338; 64,285; 84,310; 111,487
Argiope trifasciata (2)	5.9; 7.5; 9.8; 13.0	5216; 6663; 8737; 11,554	19,919; 25,444; 33,365; 44,122
Metepeira labyrinthea (5)	16.9; 21.5; 28.2; 37.3	2802; 3579; 4694; 6207	6326; 8079; 10,595; 14,011
Larinioides cornutus (4)	6.0; 7.6; 10.0; 13.2	3138; 4008; 5256; 6950	31,732; 40,527; 53,148; 70,281
Cyclosa turbinata (5)	32.2; 41.1; 53.9; 71.2	4490; 5735; 7521; 9946	7636; 9754; 12,791; 16,914
Verrucosa arenata (3)	7.1; 9.1; 11.9; 15.8	1336; 1707; 2239; 2960	4608; 5886; 7719; 10,207
Mangora maculata (2)	65.1; 83.1; 109.0; 144.2	345; 441; 578; 764	166; 212; 278; 368
Araneus pegnia (6)	8.3; 10.6; 13.9; 18.3	1697; 2168; 2843; 3759	3623; 4627; 6068; 8024
Araneus marmoreus (10)	3.6; 4.6; 6.0; 7.9	5791; 7396; 9699; 12,826	32,598; 41,637; 54,601; 72,203
Araneus bicentenarius (6)	6.0; 7.6; 10.0; 13.2	10,441; 13,335; 17,488; 23,125	74,572; 95,241; 124,902; 165,166

*Values are for contact plates of four widths: 963, 1230, 1613, and 2133 μm, respectively.

(P=0.27) along with APP (P=0.07). After removing these insignificant variables, the model contained only SVPP, which made a positive contribution, and PH2O and APP, which made negative contributions to SPP in a model with P=0.0001 and R^2=0.68. The performance of GV was worse, causing EDN, GV and RE to become insignificant (P=0.71, 0.16 and 0.44, respectively). Removing these insignificant variables produced the same three-variable model just described.

In our previous study (Opell and Hendricks, 2009) we found that dividing species into three groups (Table 1) based on unusually high or low contributions of one or two variables improved the performance of regression models (P=0.0001, $R^2 \geq 0.96$); although one or more of the original six variables were not retained in these models:

$$\text{Group 1: SPP} = (39.0259\text{EDN}) + (11.1388\text{SHAPE}) + (0.0019\text{SVPP}) - (216.1721\text{PH2O}) - (19.2173\text{RE}) + 0.5515;$$

$$\text{Group 2: SPP} = (14.5445\text{EDN}) + (3.9462\text{SHAPE}) - (0.0027\text{SVPP}) + (0.0001\text{APP}) - 78.1351;$$

$$\text{Group 3: SPP} = (34.4850\text{EDN}) + (8.1900\text{SHAPE}) - (0.0121\text{SVPP}) + (698.8896\text{PH2O}) - (31.0785\text{RE}) + (0.0013\text{APP}) - 46.0925.$$

When GA or GV was substituted for SHAPE in each of the three group models these variables made either insignificant or negative contributions to SPP and tended to render other model components insignificant. In the group 1 model both GA and GV made insignificant, negative contributions to SPP (P=0.30 and 0.66, respectively) and EDN and RE became insignificant. In the group 2 model GA made a significant negative contribution to SPP (P=0.0001). In the group 2 model GV made an insignificant, negative contribution to SPP (P=0.50) and EDN and SVPP became insignificant. In the group 3 model both GA and GV made insignificant, negative contributions to SPP (P=0.12 and 0.07, respectively) and EDN, SVPP, PH2O and RE became insignificant.

Failing to show that GA and GV were satisfactory substitutions for droplet SHAPE, we added GAPP and GVPP indices to the original six model variables in an effort to demonstrate that one or both of these granule indices made a significant, positive contribution to SPP. These attempts also failed. When GAPP was added to the model, RE became insignificant (P=0.076), but when RE was removed, the remaining variables, including GAPP, were significant (P<0.0007) in the resultant model (P=0.0001, R^2=0.88). However, the contribution of GAPP was negative:

$$\text{SPP} = (64.7698\text{EDN}) + (15.1904\text{SHAPE}) + (0.0024\text{SVPP}) - (240.2311\text{PH2O}) - (0.0005\text{APP}) - (0.0042\text{GAPP}) - 254.1989.$$

Table 3 presents the percentage contribution of these six variables as well as variables in the following two regression models, as computed from the mean values of these variables.

When GAPP was added to the group 1 model it made a small, negative contribution to SPP and all variables except APP (P=0.12) were significant (P<0.0013), as was the resulting model (P=0.0001; R^2=0.98):

$$\text{SPP} = (46.5562\text{EDN}) + (13.4446\text{SHAPE}) + (0.0022\text{SVPP}) - (211.6031\text{PH2O}) - (11.3093\text{RE}) - (0.0043\text{GAPP}) - 94.7198.$$

When GVPP was added to the group 1 model it made a small, negative contribution to SPP and all variables except APP (P=0.36)

Table 3. Percentage contribution of variables in regression models that explain stickiness per contact plate

Model variable	Composite model	Group 1 model with GAPP	Group 1 model with GVPP
EDN	99.8	96.2	106.0
SHAPE	43.5	64.7	64.2
SVPP	4.8	9.2	11.2
PH20	–31.6	–35.6	–44.3
RE	–	–24.5	–40.0
APP	–10.1	–	–
GAPP	–6.4	–9.9	–
GVPP	–	–	–7.1

EDN, effective droplet number; SHAPE, twice the focal length of a parabola defined by the lower half of a primary droplet; SVPP, total contact surface area of flattened secondary droplets on a contact plate; PH20, proportion of water in a primary droplet; RE, residual extensibility of a thread; APP, the contact surface area of flattened primary and secondary droplets on a contact plate; GAPP, total surface area of granules in primary droplets adhering to a contact plate; GVPP, total volume of granules in primary droplets adhering to a plate.

Variables that did not make a significant contribution to the regression model were excluded and a new model constructed with the remaining variables.

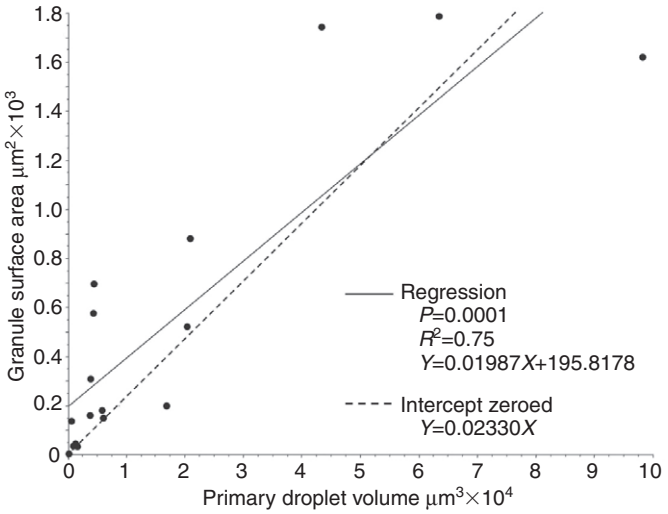

Fig. 5. Regression of granule surface area against viscous droplet volume.

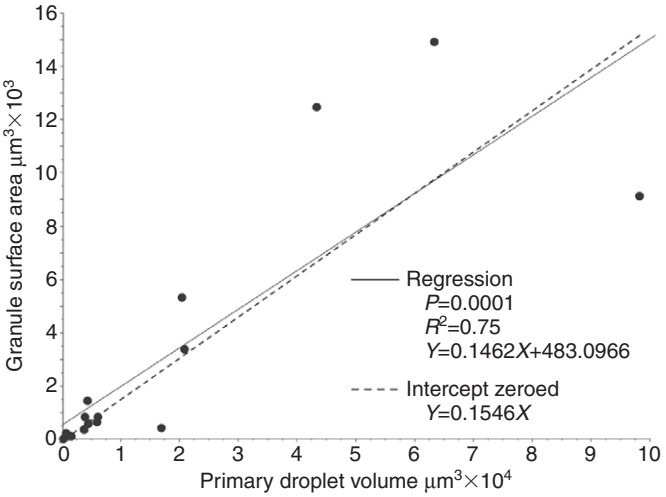

Fig. 6. Regression of granule volume against viscous droplet volume.

were significant (P<0.014), as was the resulting model (P=0.0001; R^2=0.97):

SPP = (41.7135EDN) + (12.5239SHAPE) + (0.0022SVPP) – (213.6906PH2O) – (15.0132RE) – (0.0004GVPP) – 46.4880.

GAPP and GVPP did not contribute significantly to groups 2 and 3 models.

Independent contrast analyses

Independent contrast analyses based on the values presented in Table 1 show that both granule contact surface area and granule volume are related to viscous droplet volume (P=0.0023 and 0.0003, respectively), as shown by standard regressions in Figs 5 and 6, respectively. Granule volume is approximately 15% of primary droplet volume, a value only slightly higher than that suggested by Vollrath and Tillinghast (Vollrath and Tillinghast, 1991).

DISCUSSION

A granule constitutes only a small part of the volume of a droplet and its size is directly related to droplet volume. The granules of some species (e.g. *L. cornutus*, *T. elongata* and *M. labyrinthea* in Fig. 2) seem to be formed of a large central core flanked on each end by a narrow band. Although these granules have been considered the glue of viscous threads, we were unable to demonstrate a positive relationship between granule size and thread stickiness. Instead, our results indicate that granule size is negatively related to thread stickiness. Given the robustness of the models used in these attempts and the size range of granules included, it is difficult to attribute our results solely to intraspecific variability in granule size or measurement imprecision. However, we acknowledge the possibility that these factors may have had an impact. A violation of our assumption that the granules of all species' threads flatten to a similar degree would probably have little effect on our measurements of granule area, although it would affect our estimation of granule volume.

The relative humidity (RH) under which threads are produced can affect both the speed at which droplets coalesce and the features of their granules (Vollrath and Tillinghast, 1991). As all threads used in this study were produced under natural conditions, we do not have information about the RH under which droplets and granules formed. However, it is unlikely that these values were as extreme as the 9% and 90% RHs used by Vollrath and Tillinghast (Vollrath and Tillinghast, 1991) to demonstrate the effect of humidity on thread properties. Diet also affects the composition of viscous threads (Townley et al., 2006), another factor that our study cannot address.

We do not suggest that our results refute the conclusion that glycoprotein glue within viscous droplets is responsible for the adhesion of viscous threads (Vollrath and Tillinghast, 1991; Tillinghast et al., 1993). Indeed, it is difficult to suggest an alternative explanation. However, we believe that our results indicate that viscous droplets are more highly structured than previously thought and that the small, distinct granule visible at the center of each droplet is not this glycoprotein glue, but rather an anchor that secures the surrounding transparent glycoprotein glue to the axial fibers of the thread. Thus, we hypothesize that a viscous droplet is formed of three regions: a small central, opaque anchoring granule, a larger surrounding, transparent glycoprotein glue region, and a more fluid outer covering that extends onto interdroplet regions (Fig. 7). This organization would allow droplets to generate adhesion,

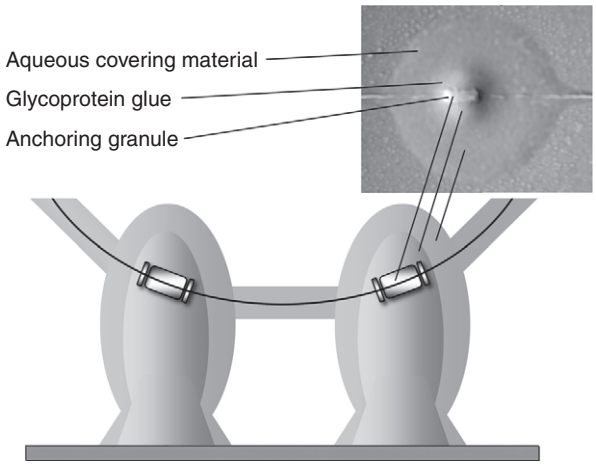

Fig. 7. Hypothesized model of droplet organization, showing a small central anchoring granule surrounded by a large glycoprotein glue region, which is covered by fluid.

elongate under a load, transfer force to the axial fibers, and resist slippage on the axial fibers.

Some droplet images (e.g. *A. aurantia*, *T. gemmosum* and *V. arenata* in Fig. 2) seem to show these three regions. This model would also resolve the paradox of why, if granules are responsible for thread adhesion, they constitute such a small part of the droplet volume. This hypothesis is consistent with the small negative contribution that granule size makes to thread stickiness in several of our models (Table 3). If the granule serves an anchoring function and does not contribute to adhesion, its volume must be subtracted from the total volume of the thread to more accurately account for the adhesive components of the droplet.

When *A. marmoreus* droplets were examined histologically (Peters, 1995) they appeared to be formed of three regions: a fairly uniform dense outer layer, a large middle region consisting of vesicles containing less dense material, and a smaller inner region formed of smaller, denser vesicles in which the two axial fibers were embedded. We used ImageJ to measure the droplet shown in fig. 3 of Peters (Peters, 1995) and found that the outer region, middle region, inner region and axial fibers were 28%, 53.9%, 13.7% and 4.3%, respectively, of the total cross sectional area of the droplet. Although vesicular and not highly consolidated, the middle and inner regions appear to correspond in both position and size to our hypothesized glycoprotein glue and granule regions, respectively, of a droplet. As each posterior lateral spinneret has two aggregate gland spigots, one gland may contribute glycoprotein glue and the other gland granule material, with the combined aqueous carrier material of both glands forming the droplet's outer covering.

From the time that the droplets on a viscous thread coalesce after being spun until they contact a surface and elongate under a load, a viscous thread exhibits many characteristics of a self-organizing system with emergent properties. That is, interactions among its components play a major role in establishing its structural and functional organization (Camazine et al., 2001) and, once configured, these components create a dynamic system with new properties that cannot be predicted from the behavior of its individual components (Aziz-Alaoui and Bertelle, 2006).

We propose that when droplets flatten against a surface and then elongate under a load, the vesicles in their central and inner regions coalesce and their proteins condense and polymerize to confer their anchoring, adhesive and extensile properties. As droplets extend, a swollen region remains associated with the axial fibers and this is probably the granule (Fig. 3). In the later stages of droplet elongation small sub droplets form on the extending droplet and migrate toward the axial fibers. Thus, it appears that, after being flattened, a droplet becomes less fluid and assumes a stiffer, plastic state, such as might occur if its proteins were polymerized by elongation.

When we pressed a sliver of broken coverslip against *A. aurantia* and *A. marmoreus* threads and then pulled it away, most elongating droplets pulled free of the glass rather than rupturing. These droplets then reformed around the axial fibers with the size of many droplets remaining similar to their original configuration. It is challenging to observe the interior of suspended droplets because of their small sizes, their ability to function as lenses, and the fact that droplets are suspended far above the microscope stage, making Koehler Illumination difficult. However, in *A. marmoreus*, which has the largest droplets of all the species that we studied, contact and elongation do appear to change the internal organization of droplets (Fig. 8). In these images the droplet's convex surface magnifies the axial fibers that extend through the droplet and in unused droplets show a dense sheath surrounding the axial fibers. By contrast, not only is this sheath deformed in droplets that have pulled free of a surface, but also a slightly denser oval, which we believe to be the granule, becomes visible at the droplet's center. We believe that this faint appearance, when contrasted with the distinct appearance of a granule that has contacted a surface, supports the hypothesis that contact physically and perhaps also chemically alters the granule's material and fully imparts its functional characteristics.

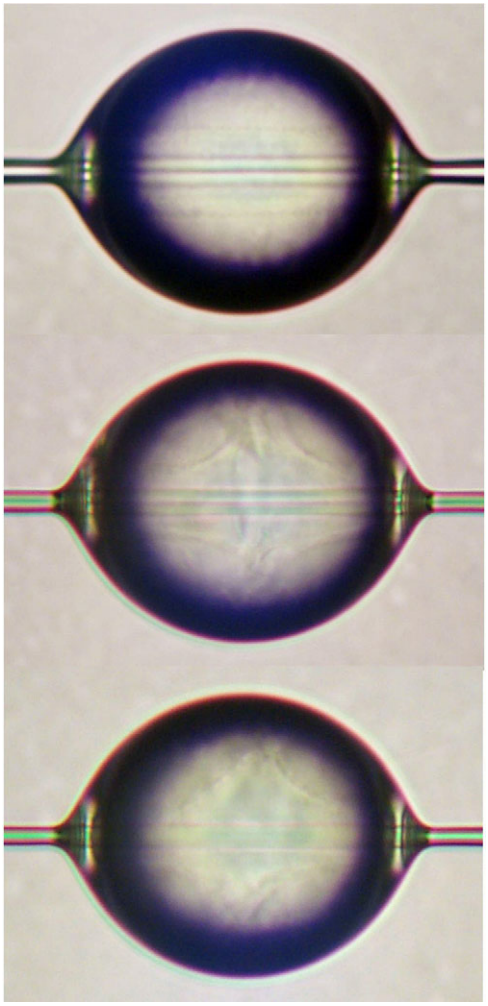

Fig. 8. Viscous droplets of *A. marmoreus* before contacting a surface (top), after being pulled from an acetate surface (middle), and after being pulled from a glass surface (bottom).

LIST OF ABBREVIATIONS

APP	the contact surface area of flattened primary and secondary droplets on a contact plate
DL	primary droplet length
DW	primary droplet width
EDN	the total droplet equivalents that contribute to a thread's stickiness on a contact plate
GA	contact surface area of a granule in a primary droplet
GAPP	total surface area of granules in primary droplets adhering to a contact plate
GL	length of a granule in a primary droplet
GV	volume of a granule in a primary droplet
GVPP	total volume of granules in primary droplets adhering to a plate
GW	width of a granule in a primary droplet

PDPP	primary droplets per contact plate
PH2O	proportion of water in a primary droplet
PV	volume of a primary droplet
RE	residual extensibility of a thread
SDPP	number of secondary droplets per contact plate
SHAPE	twice the focal length of a parabola defined by the lower half of a primary droplet
SVPP	total secondary droplet volume per contact plate
T	thickness of a flattened primary droplet, determined by dividing its PV by its flattened area

ACKNOWLEDGEMENTS

Andrea Burger, Brian Segal, Mike Leonard, Lindsay Neist, Brian Markley, Chip Hannum, Genine Lipkey, Kaitlin Flora, and Steve Vito helped collect and photograph threads. Harold Schwend assisted with granule measurements. This study was supported by National Science Foundation grant IOB-0445137.

REFERENCES

Aziz-Alaoui, M. A. and Bertelle, C. E. (2006). *Emergent Properties in Natural and Artificial Dynamical Systems*. Berlin: Springer-Verlag,

Blackledge, T. A. and Eliason, C. M. (2007). Functionally independent components of prey capture are architecturally constrained in spider orb webs. *Biol. Lett.* **3**, 456-458.

Blackledge, T. A., Scharff, N., Coddington, J., Szüts, T., Wenzel, J., Hayashi, C. and Agnarsson, I. (2009). Reconstructing web evolution and spider diversification in the molecular era. *Proc. Natl. Acad. Sci. USA* **106**, 5229-5234.

Camazine, S., Deneubourg, J., Franks, N., Sneyd, J., Theraula, G. and Bonabeau, E. (2001). *Self-Organization in Biological Systems*. Princeton, N.J: Princeton University Press.

Chacón, P. and Eberhard, W. G. (1980). Factors affecting numbers and kinds of prey caught in artificial spider webs with considerations of how orb-webs trap prey. *Bull. Br. Arachnol. Soc.* **5**, 29-38.

Coddington, J. A. and Levi, H. W. (1991). Systematics and evolution of spiders (Araneae). *Ann. Rev. Ecol. Syst.* **22**, 565-592.

Eberhard, W. G. (1986). Effect of orb-web geometry on prey interception and retention. In *Spiders: Webs, Behavior, and Evolution* Evolution (ed. W. A. Shear). pp. 70-100. Stanford: Stanford University Press.

Eberhard, W. G. (1990). Function and phylogeny of spider webs. *Ann. Rev. Ecol. Syst.* **21**, 341-372.

Eberhard, W. G. and Pereira, F. (1993). Ultrastructure of cribellate silk of nine species in eight families and possible taxonomic implications. (Araneae: Amaurobiidae, Deinopidae, Desidae, Dictynidae, Filistatidae, Hypochilidae, Stiphidiidae, Tengellidae). *J. Arachnol.* **21**, 161-174.

Gosline, J. M., Pollak, C. C., Guerette, P. A., Cheng, A., DeMont, M. E. and Denny, M. W. (1994). Elastomeric network models for the frame and viscid silks from the orb web of the spider *Araneus diadematus*. In *Silk Polymers, Materials Science and Biotechnology* (eds D. Kaplan, W. Adams, B. Farmer and C. Viney), pp. 328-341. Washington, DC: American Chemical Society.

Griswold, C. E., Coddington, J. A., Hormiga, G. and Scharff, N. (1998). Phylogeny of the orb-web building spiders (Araneae, Orbiculariae: Deinopoidea, Araneoidea). *Zool. J. Linn. Soc.* **123**, 1-99.

Griswold, C. E., Ramírez, M. J., Coddington, J. A. and Platnick, N. I. (2005). Atlas of phylogenetic data for eneelegyne spiders (Araneae: Araneomorphae: Entelegynae) with comments on their phylogeny. *Proc. Cali. Acad. Sci.* **56**, Suppl II, 1-324.

Hu, X., Yuan, J., Wang, X., Vasanthavada, K., Falick, A. M., Jones, P. R., La Mattina, C. and Vierra, C. A. (2007). Analysis of aqueous glue coating proteins on the silk fibers of the cob weaver, *Latrodectus hesperus*. *Biochemistry* **46**, 3294-3303.

Levi, H. W. (1971). The *Diadematus* group of the orb-weaver genus *Araneus* North of Mexico (Araneae: Araneidae). *Bull. Mus. Comp. Zool.* **141**, 131-179.

Levi, H. W. (1973). Small orb-weavers of the genus *Araneus* North of Mexico (Araneae: Araneidae). *Bull. Mus. Comp. Zool.* **145**, 473-552.

Maddison, W. P. and Maddison, D. R. (2008). Mesquite: a modular system for evolutionary analysis. Version 2.5 http://mesquiteproject.org.

Midford, P. E., Garland, T. J. and Maddison, W. P. (2005). PDAP: PDTREE package for Mesquite, version 1.07. http://mesquiteproject.org/pdap_mesquite/.

Opell, B. D. (1994a). Factors governing the stickiness of cribellar prey capture threads in the spider family Uloboridae. *J. Morphol.* **221**, 111-119.

Opell, B. D. (1994b). Increased stickiness of prey capture threads accompanying web reduction in the spider family Uloboridae. *Funct. Ecol.* **8**, 85-90.

Opell, B. D. (1996). Functional similarities of spider webs with diverse architectures. *Am. Nat.* **148**, 630-648.

Opell, B. D. (1999). Changes in spinning anatomy and thread stickiness associated with the origin of orb-weaving spiders. *Biol. J. Linn. Soc.* **68**, 593-612.

Opell, B. D. and Hendricks, M. L. (2007). Adhesive recruitment by the viscous capture threads of araneoid orb-weaving spiders. *J. Exp. Biol.* **210**, 553-560.

Opell, B. D. and Hendricks, M. L. (2009). The adhesive delivery system of viscous capture threads spun by orb-weaving spiders. *J. Exp. Biol.* **212**, 3026-3034.

Opell, B. D., Markley, B. J., Hannum, C. D. and Hendricks, M. L. (2008). The contribution of axial fiber extensibility to the adhesion of viscous capture threads spun by orb-weaving spiders. *J. Exp. Biol.* **211**, 2243-2251.

Peters, H. M. (1984). The spinning apparatus of Uloboridae in relation to the structure and construction of capture threads (Arachnida, Araneida). *Zoomorphology* **104**, 96-104.

Peters, H. M. (1986). Fine structure and function of capture threads. In *Ecophysiology of Spiders* (ed. W. Nentwig), pp. 187-202. New York: Springer Verlag.

Peters, H. M. (1992). On the spinning apparatus and structure of the capture threads of *Deinopis subrufus* (Araneae, Deinopidae). *Zoomorphology* **112**, 27-37.

Peters, H. M. (1995). Ultrastructure of orb spiders' gluey capture threads. *Naturwissenschaften* **82**, 380-382.

Platnick, N. I. (2009). The World Spider Catalog, Version 10.0. New York: American Museum of Natural History. Online at http://research.amnh.org/entomology/spiders/catalog/index.html.

Savage, K. N. and Gosline, J. M. (2008). The role of proline in the elastic mechanism of hydrated spider silks. *J. Exp. Biol.* **211**, 1948-1957.

Scharff, N. and Coddington, J. A. (1997). A phylogenetic analysis of the orb-weaving spider family Araneidae (Arachnida, Araneae). *Zool. J. Linn. Soc.* **120**, 355-434.

Tillinghast, E. K., Townley, M. A., Wight, T. N., Uhlenbruck, G. and Janssen, E. (1993). The adhesive glycoprotein of the orb web of *Argiope aurantia* (Araneae, Araneidae). *Materials Research Society Symposium Proceedings* **292**, 9-23.

Townley, M. A., Bernstein, D. T., Gallangher, K. S. and Tillinghast, E. K. (1991). Comparative study of orb web hygroscopicity and adhesive spiral composition in three araneid spiders. *J. Exp. Zool.* **259**, 154-165.

Townley, M. A., Tillinghast, E. K. and Neefus, C. D. (2006). Changes in composition of spider orb web sticky droplets with starvation and web removal, and synthesis of sticky droplet compounds. *J. Exp. Biol.* **209**, 1463-1486.

Vollrath, F. (1992). Spider webs and silks. *Sci. Am.* **266**, 70-76.

Vollrath, F. and Tillinghast, E. K. (1991). Glycoprotein glue beneath a spider web's aqueous coat. *Naturwissenschaften* **78**, 557-559.

Vollrath, F., Fairbrother, W. J., Williams, R. J. P., Tillinghast, E. K., Bernstein, D. T., Gallagher, K. S. and Townley, M. A. (1990). Compounds in the droplets of the orb spider's viscid spiral. *Nature* **345**, 526-528.

Work, R. W. (1981). A comparative study of the supercontraction of major ampullate spider fibers of orb-weaving spiders (Araneae). *J. Arachnol.* **9**, 299-308.

Work, R. W. (1982). A physico-chemical study of the supercontraction of spider major ampullate silk fibers. *Text. Res. J.* **52**, 349-356.